3 Y. Matsuo, H. Okada, M. Maruyama, H. Sato, H. Tobita, Y. Ono, K. Omote, K. Kawachi and Y. Kasama, *Org. Lett.*, 2012, **14**, 3784–3787.
4 L. Y. Chiang, F.-J. Lu and J.-T. Lin, *J. Chem. Soc., Chem. Commun.*, 1995, 1283–1284.
5 H. Aoshima, K. Kokubo, S. Shirakawa, M. Ito, S. Yamana and T. Oshima, *Biocontrol Sci.*, 2009, **14**, 69–72.
6 J. Gao, L. Wang, K. M. Folta, V. Krishna, W. Bai, P. Indeglia, A. Georgieva, H. Nakamura, B. Koopman and B. Moudgil, *PLoS One*, 2011, **6**, e19976.
7 Y. Saitoh, H. Mizuno, L. Xiao, S. Hyoudou, K. Kokubo and N. Miwa, *Mol. Cell. Biochem.*, 2012, **366**, 191–200.
8 Z. Chen, L. Ma, Y. Liu and C. Chen, *Theranostics*, 2012, **2**, 238–250.
9 L. Y. Chiang, L.-Y. Wang, J. W. Swirczewski, S. Soled and S. Cameron, *J. Org. Chem.*, 1994, **59**, 3960–3968.
10 N. S. Schneader, A. D. Darwish, H. W. Kroto, R. Taylor and D. R. M. Walton, *J. Chem. Soc., Chem. Commun.*, 1994, 463–464.
11 S. Wang, P. He, J.-M. Zhang, H. Jiang and S.-Z. Zhu, *Synth. Commun.*, 2005, **35**, 1803–1807.
12 A. Arrais and E. Diana, *Fullerenes, Nanotubes, Carbon Nanostruct.*, 2003, **11**, 35–46.
13 J. Li, A. Takeuchi, M. Ozawa, X. Li, K. Saigo and K. Kitazawa, *J. Chem. Soc., Chem. Commun.*, 1993, 1784–1785.
14 K. Kokubo, K. Matsubayashi, H. Tategaki, H. Takada and T. Oshima, *ACS Nano*, 2008, **2**, 327–333.
15 K. Kokubo, S. Shirakawa, N. Kobayashi, H. Aoshima and T. Oshima, *Nano Res.*, 2011, **4**, 204–215.
16 G. Zhang, Y. Liu, D. Liang, L. Gan and Y. Li, *Angew. Chem., Int. Ed.*, 2010, **49**, 5293–5295.
17 M. Mikawa, H. Kato, M. Okumura, M. Narazaki, Y. Kanazawa, N. Miwa and H. Shinohara, *Bioconjugate Chem.*, 2001, **12**, 510–514.
18 B. Sitharaman, R. B. Bolskar, I. Rusakova and L. J. Wilson, *Nano Lett.*, 2004, **4**, 2373–2378.
19 H. Ueno, Y. Nakamura, N. Ikuma, K. Kokubo and T. Oshima, *Nano Res.*, 2012, **6**, 558–564.
20 R. H. Seubold, Jr, *J. Org. Chem.*, 1956, **21**, 156–160.
21 H. Thomann, M. Bernardo and G. P. Miller, *J. Am. Chem. Soc.*, 1992, **114**, 6593–6594.
22 F. Cataldo, *Spectrochim. Acta*, 1995, **51A**, 405–414.
23 S. P. Solodovnikov, *Russian Chemical Bulletin*, 1998, **47**, 2302–2304.
24 R. D. Webster and G. A. Heath, *Phys. Chem. Chem. Phys.*, 2001, **3**, 2588–2594.
25 S. G. Kukolich and D. R. Huffman, *Chem. Phys. Lett.*, 1991, **182**, 263–265.
26 S. Fukuzumi, T. Suenobu, T. Urano and K. Tanaka, *Chem. Lett.*, 1997, 875–876.
27 K. Tanaka, H. Ago, Y. Matsuura, T. Kuga, T. Yamabe, S. Yuda, Y. Hato and N. Ando, *Synth. Met.*, 1997, **89**, 133–139.
28 C. D. Johnson, *Chem. Rev.*, 1975, **75**, 755–765.
29 B. Giese, *Angew. Chem., Int. Ed. Engl.*, 1977, **16**, 125–136.
30 A. Pross, in *Advances in Physical Organic Chemistry*, ed. V. Gold and D. Bethell, Academic Press, London, New York, San Francisco, 1977, vol. 14, p. 69–132.
31 Y. Wada, S. Totoki, M. Watanabe, N. Moriya, Y. Tsunazawa and H. Shimaoka, *Opt. Express*, 2006, **14**, 5755–5776.

ChemComm

RSC Publishing

COMMUNICATION

# Ionic conductivity of $[Li^+@C_{60}](PF_6^-)$ in organic solvents and its electrochemical reduction to $Li^+@C_{60}^{\bullet -}$

Cite this: *Chem. Commun.*, 2013, **49**, 7376

Received 24th May 2013,
Accepted 26th June 2013

DOI: 10.1039/c3cc43901a

www.rsc.org/chemcomm

Hiroshi Ueno,[a] Ken Kokubo,*[a] Yuji Nakamura,[a] Kei Ohkubo,[b] Naohiko Ikuma,[a] Hiroshi Moriyama,[c] Shunichi Fukuzumi[bd] and Takumi Oshima[a]

**The ionic conductivity of $[Li^+@C_{60}](PF_6^-)$ was measured in *o*-dichlorobenzene, and found to be higher than that of $TBA^+PF_6^-$. Electrochemical reduction of $[Li^+@C_{60}](PF_6^-)$ without any supporting electrolyte gave the monovalent radical anion $Li^+@C_{60}^{\bullet -}$, as confirmed by the characteristic ESR signal and NIR absorption band.**

Lithium-cation-encapsulated [60]fullerene $Li^+@C_{60}$, which was first isolated as the $[Li^+@C_{60}](SbCl_6^-)$ salt, is the only known endohedral metallo[60]fullerene with 100% encapsulation ratio, and its structure has been established by single crystal X-ray analysis.[1–3] It has attracted growing attention because of its unique properties such as stronger electron acceptability than pristine $C_{60}$ and high reactivities in photoinduced electron transfer and regioselective multihydroxylation.[4–8] The most remarkable property of the $[Li^+@C_{60}]$ salt is its high ionicity resulting from the encapsulated lithium cation. Although this ionic nature of $[Li^+@C_{60}](PF_6^-)$ is stated to be responsible for its rock-salt-type crystal structure,[2] no other details of the effects of ionicity have been reported so far.

The fullerene radical anion has been recognised as an intriguing material because of its unique electronic properties such as (super)conductivity and ferromagnetism.[9–12] In addition, the radial anion can serve as an important reaction intermediate for various unique chemical modifications of the fullerene cage.[13] Although many methods for the preparation of empty $C_{60}$ radical anion salts have been reported,[14] studies on endohedral fullerene radical anions are relatively stagnant.

We herein report the high ionic conductivity of $[Li^+@C_{60}](PF_6^-)$ in organic solvents, which has enabled a facile electrochemical synthesis of the radical anion $(Li^+@C_{60}^{\bullet -})$ without any supporting electrolyte.

The ionic conductivity measurements were performed in *o*-dichlorobenzene (*o*-DCB) and benzonitrile (PhCN) since $[Li^+@C_{60}](PF_6^-)$ showed sufficient solubility and electrochemical stability in these solvents.† The molar conductivity $\Lambda$ is defined in eqn (1), where $\kappa$ is the measured conductivity at each concentration ($c$). The $\Lambda$ values for various concentrations

$$\Lambda = \kappa/c \quad (1)$$

of $[Li^+@C_{60}](PF_6^-)$ are shown in Fig. 1 and listed in Table 1, together with those of tetra-*n*-butylammonium hexafluorophosphate $(TBA^+PF_6^-)$, which is commonly used as a supporting electrolyte in organic solvents. The exponential change in $\Lambda$ with $c^{1/2}$ indicated that $[Li^+@C_{60}](PF_6^-)$ itself acted as a supporting electrolyte. As pristine $C_{60}$ showed no ionic conductivity under the same conditions, the observed conductivity was regarded as a unique feature of the ion-encapsulated fullerene. The observed

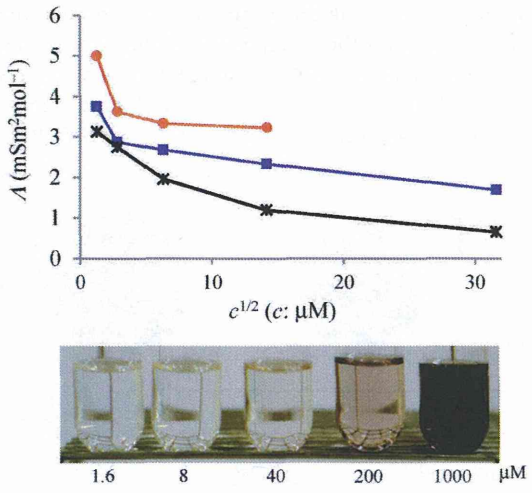


**Fig. 1** Molar conductivity of $[Li^+@C_{60}](PF_6^-)$ measured in PhCN (red circles) and o-DCB (blue squares) solutions containing various concentrations of $[Li^+@C_{60}](PF_6^-)$ at 298 K. The black line is the result of $TBA^+PF_6^-$ measured as a reference (asterisks). The picture shows the various concentrations of $[Li^+@C_{60}](PF_6^-)$ in *o*-DCB solutions.

[a] *Division of Applied Chemistry, Graduate School of Engineering, Osaka University, 2-1 Yamadaoka, Suita, Osaka 565-0871, Japan. E-mail: kokubo@chem.eng.osaka-u.ac.jp; Fax: +81-6-6879-4593; Tel: +81-6-6879-4592*

[b] *Department of Material and Life Science, Graduate School of Engineering, Osaka University, and ALCA, Japan Science and Technology (JST), Suita, Osaka 565-0871, Japan*

[c] *Department of Chemistry, Faculty of Science, Toho University, 2-2-1 Miyama, Funabashi, Chiba 274-8510, Japan*

[d] *Department of Bioinspired Science, Ewha Womans University, Seoul, 120-750, Korea*

**Table 1** Ionic conductivities of $[Li^+@C_{60}](PF_6^-)$ and $TBA^+PF_6^-$ measured in *o*-DCB at 298.0 K

| $c$/μM | $\kappa$/mS m$^{-1}$ | $\Lambda$/mS m$^{-2}$ mol$^{-1}$ |
|---|---|---|
| $[Li^+@C_{60}](PF_6^-)$ | | |
| 1.6 | 0.006 (0.008)[a] | 3.75 (5.00)[a] |
| 8 | 0.023 (0.029)[a] | 2.88 (3.63)[a] |
| 40 | 0.107 (0.133)[a] | 2.68 (3.33)[a] |
| 200 | 0.466 (0.646)[a] | 2.33 (3.23)[a] |
| 1000 | 1.688 (—[b])[a] | 1.69 (—[b])[a] |
| $TBA^+PF_6^-$ | | |
| 1.6 | 0.005 | 3.13 |
| 8 | 0.022 | 2.75 |
| 40 | 0.078 | 1.95 |
| 200 | 0.238 | 1.19 |
| 1000 | 0.649 | 0.50 |
| Pristine $C_{60}$ | | |
| Any | 0.000 | 0.00 |

[a] Values in parentheses are measured in PhCN. [b] Not determined due to the solubility limitation.

ionic conductivity of $[Li^+@C_{60}](PF_6^-)$ was higher than that of $TBA^+PF_6^-$, indicating the weak interaction between the counter anion $PF_6^-$ and encapsulated $Li^+$ even in such less polar solvents.

To discuss the ionizability of $[Li^+@C_{60}](PF_6^-)$, the electrostatic potential of the $[Li^+@C_{60}]$ cation and the distance between the cation and the $PF_6^-$ anion at the most stable position were calculated by the density functional theory (DFT) at the B3LYP/6-31G* level. The result showed that the positive charge of the $[Li^+@C_{60}]$ cation was not only located on the encapsulated $Li^+$ but also strongly delocalised on the carbon atoms of the $C_{60}$ cage. Because of the thermal motion of the encapsulated $Li^+$ in the $C_{60}$ cage, the charge delocalization might be more dynamically significant.[2] Furthermore, the Li–P distance of $[Li^+@C_{60}](PF_6^-)$ was calculated to be 5.65 Å, which was much longer than that in $LiPF_6$ (2.63 Å). This difference implied that the positional relationship observed between $Li^+$ and $PF_6^-$ in $[Li^+@C_{60}](PF_6^-)$ is unusual in common ion pairs, indicating that the electrostatic attractive force between the $[Li^+@C_{60}]$ cation and $PF_6^-$ is weak due to the delocalised positive charge on the $C_{60}$ cage and the distance limitation by this cage. This result is consistent with the previous report that the encapsulated $Li^+$ is in thermal motion at around room temperature even if the $[Li^+@C_{60}]$ cation forms an ion pair with $PF_6^-$.[2]

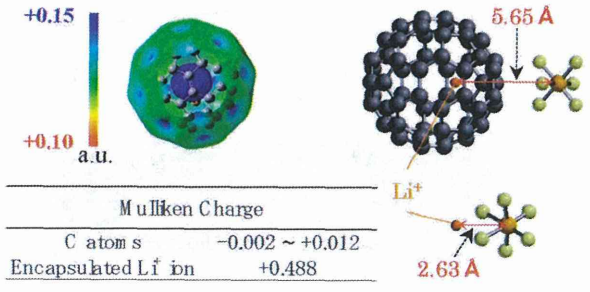


**Fig. 2** Electrostatic potential of the $[Li^+@C_{60}]$ cation and the distance between encapsulated $Li^+$ and outer $PF_6^-$ obtained by the theoretical calculation (B3LYP/6-31G* method), the distances between $Li^+$ and P for $Li^+@C_{60}$ and $LiPF_6$, and the Mulliken charges on C and $Li^+$ atoms of the $[Li^+@C_{60}]$ cation.

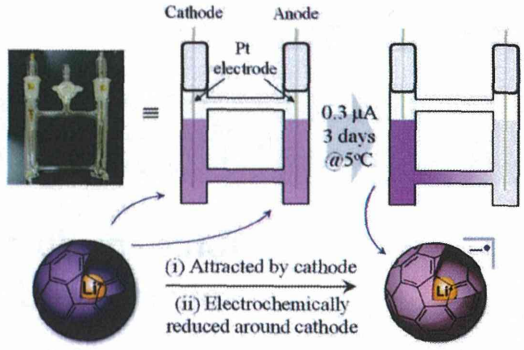


**Fig. 3** Pattern diagram of the electrochemical synthesis of $Li^+@C_{60}^{\bullet-}$.

Moreover, the solvation effect is also important for the ion pair formation.[15] Because $C_{60}$ is a π-conjugated molecule, there must be strong π–π interaction between the cage and the aromatic solvent molecules, and the solvation can stabilize the ionized $[Li^+@C_{60}]$ cation.[16] Thus, $[Li^+@C_{60}](PF_6^-)$ tends to ionize, showing ionic conductivity, to be used as a unique electrolyte which, despite its high ionicity, can be used in low-polarity aromatic solvents. Incidentally, the higher value of $\Lambda$ in PhCN than that in *o*-DCB was explained by the difference in the relative permittivity ($\varepsilon_r$) between PhCN ($\varepsilon_r$ = 25.2) and *o*-DCB (9.93).[17]

Based on the above results, we attempted at synthesis of the $Li^+$-encapsulated fullerene radical anion electrochemically without using any supporting electrolyte. All the synthetic process was carried out under $N_2$ atmosphere. The synthetic scheme is shown in Fig. 3. An *o*-DCB solution of $[Li^+@C_{60}](PF_6^-)$ (0.25 mg mL$^{-1}$, 0.29 μM) was set in an H-type cell, cooled to 278 K, and electrolyzed using a Pt electrode at a constant current (0.3 μA) for 3–4 days. The homogeneous purple solution gradually became gradated because of ion conduction by the $[Li^+@C_{60}]$ cation and $PF_6^-$. The cation was electrochemically reduced at the cathode, and a monovalent radical anion of $Li^+$-encapsulated fullerene $Li^+@C_{60}^{\bullet-}$ was selectively formed.

The generated $Li^+@C_{60}^{\bullet-}$ was characterised by UV-vis-NIR and ESR spectroscopy. $^7Li$ and $^{13}C$ NMR, dynamic light scattering (DLS), and ζ potential distribution measurements did not furnish meaningful signals/results, probably because of the low concentration of the target species, in addition to paramagnetic relaxation. The UV-vis-NIR spectra of the solution collected from the cathode side after 3 days are shown in Fig. 4, along with the spectrum of the starting $[Li^+@C_{60}](PF_6^-)$ solution. The absorption maximum observed at 1035 nm was clearly assignable to the monovalent radical anion of the $Li^+$-encapsulated $C_{60}$.[7,8] The generation of $Li^+@C_{60}^{\bullet-}$ was also confirmed by the ESR spectrum (Fig. 5). The observed $g$ value (2.00058) clearly indicated that the monovalent radical anion was exclusively produced through one-electron reduction. At 77 K, the thermal motion of the encapsulated $Li^+$ may stop, and thus, the spectrum showed a sharp signal. The calculated spin density of $Li^+@C_{60}^{\bullet-}$ for the optimised structure indicated that the delocalised spin density is somewhat close to the encapsulated $Li^+$. However, because of the small hyperfine coupling constant of the Li species, the interaction between the encapsulated $Li^+$ and

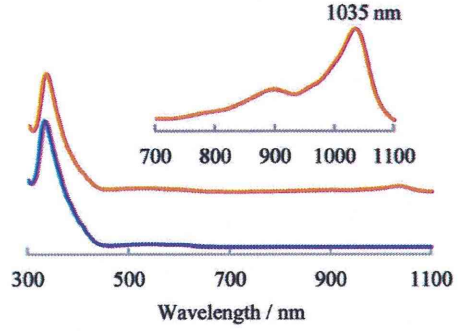


**Fig. 4** UV-vis-NIR absorption spectra of the product solution by electrochemical reduction of $[Li^+@C_{60}](PF_6^-)$ (red line) and starting $[Li^+@C_{60}](PF_6^-)$ solution (blue line) in *o*-DCB. The inset shows the expanded view of the NIR region of the spectrum of the product.

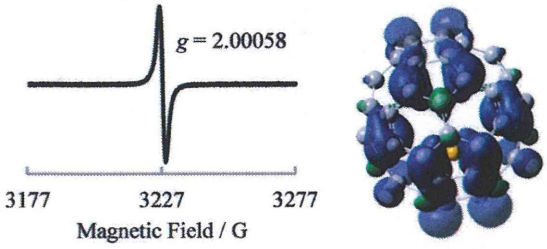


**Fig. 5** ESR spectrum of the product measured at 77 K (left) and calculated spin density (B3LYP/6-31G* method) of $Li^+@C_{60}^{\bullet-}$ in the optimised structure (right).

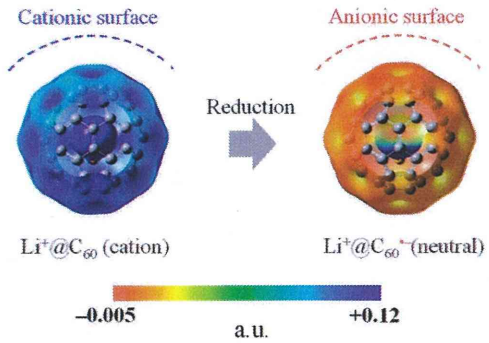


**Fig. 6** Calculated electrostatic potential (B3LYP/6-31G* method) of $Li^+@C_{60}$ (left) and $Li^+@C_{60}^{\bullet-}$ (right). The left figure is different from Fig. 2 only in the potential range. $Li^+@C_{60}^{\bullet-}$ had a slightly negative potential on the $C_{60}$ cage (~0.022). In order to simplify the map, the range was set in +0.002 to +0.12.

the spin centre could not be evidenced from the spectrum. Although the ζ potentials of the starting $[Li^+@C_{60}](PF_6^-)$ and the resulting $Li^+@C_{60}^{\bullet-}$ could not be compared because of the above reasons, the two species could be clearly distinguished from each other on the basis of the calculated electrostatic potential (Fig. 6). This result indicated that the chemical reactivities of the two types of $Li^+$-encapsulated fullerenes, the external-counter-anion-type $[Li^+@C_{60}](PF_6^-)$ and the cation-encapsulated-anion-type $Li^+@C_{60}^{\bullet-}$, are much different, and hence, $Li^+@C_{60}^{\bullet-}$ is a potential nucleophilic reactant for unique chemical transformations.

In conclusion, the ionic conductivity of $Li^+$-encapsulated [60]fullerene $[Li^+@C_{60}](PF_6^-)$ was measured in two organic solvents, *o*-DCB and PhCN. $[Li^+@C_{60}](PF_6^-)$ showed higher ionic conductivity than $TBA^+PF_6^-$, indicating the possibility of electrochemical applications even in the absence of any supporting electrolyte. Furthermore, the $Li^+$-encapsulated [60]fullerene monovalent radical anion $Li^+@C_{60}^{\bullet-}$ was synthesised selectively by a very facile electrochemical method. Further studies on the use of anion-exchanged $[Li^+@C_{60}]$, application of $[Li^+@C_{60}](PF_6^-)$ as a unique electrolyte, and derivatisation *via* the anion species are now in progress, in addition to the synthesis and characterization of multivalent anions.

This work was supported by Grant-in-Aid for Exploratory Research (No. 23651111 to K.K.; No. 23750014 to K.O.; No. 23550211 to H.M. & 23108010 to S.F.) from JSPS, Japan, Health Labour Sciences Research Grants from MHLW, Japan, and a WCU project (R31-2008-000-10010-0) through KOSEF/MEST, Korea.

## References

† General procedure: $[Li^+@C_{60}](PF_6^-)$ was obtained from Idea International Corporation and purified by recrystallization from chlorobenzene/acetonitrile. All other reagents were commercially available and used without further purification. Ionic conductivity measurement was performed using a HORIBA ES-51 under $N_2$ atmosphere. UV-vis-NIR spectra were recorded on a Shimadzu UV-1800 spectrometer. The ESR spectrum was measured on a JEOL JES-FA100. A YAZAWA CS-12Z constant current regulator was used for electrochemical synthesis of $Li^+@C_{60}^{\bullet-}$.

1 S. Aoyagi, E. Nishibori, H. Sawa, K. Sugimoto, M. Takata, Y. Miyata, R. Kitaura, H. Shinohara, H. Okada, T. Sakai, Y. Ono, K. Kawachi, K. Yokoo, S. Ono, K. Omote, Y. Kasama, S. Ishikawa, T. Komuro and H. Tobita, *Nat. Chem.*, 2010, **2**, 678.
2 S. Aoyagi, Y. Sado, E. Nishibori, H. Sawa, H. Okada, H. Tobita, Y. Kasama, R. Kitaura and H. Shinohara, *Angew. Chem., Int. Ed.*, 2012, **51**, 3377.
3 H. Okada, T. Komuro, T. Sakai, Y. Matsuo, Y. Ono, K. Omote, K. Yokoo, K. Kawachi, Y. Kasama, S. Ono, R. Hatakeyama, T. Kaneko and H. Tobita, *RSC Adv.*, 2012, **2**, 10624.
4 H. Ueno, Y. Nakamura, N. Ikuma, K. Kokubo and T. Oshima, *Nano Res.*, 2012, **6**, 558.
5 H. Ueno, K. Kokubo, E. Kwon, Y. Nakamura, N. Ikuma and T. Oshima, *Nanoscale*, 2013, **5**, 2317.
6 Y. Matsuo, H. Okada, M. Maruyama, H. Sato, H. Tobita, Y. Ono, K. Omote, K. Kawachi and Y. Kasama, *Org. Lett.*, 2012, **14**, 3784.
7 S. Fukuzumi, K. Ohkubo, Y. Kawashima, D. S. Kim, J. S. Park, A. Jana, V. M. Lynch, D. Kim and J. L. Sessler, *J. Am. Chem. Soc.*, 2011, **133**, 15938.
8 (*a*) K. Ohkubo, Y. Kawashima and S. Fukuzumi, *Chem. Commun.*, 2012, **48**, 4314; (*b*) Y. Kawashima, K. Ohkubo and S. Fukuzumi, *J. Phys. Chem. A*, 2012, **116**, 8942.
9 K. Tanigaki, I. Hirosawa, T. W. Ebbesen, J. Mizuki, Y. Shimakawa, Y. Kubo, J. S. Tsai and S. Kuroshima, *Nature*, 1992, **356**, 419.
10 A. Y. Ganin, Y. Takabayashi, P. Jeglič, D. Arčon, A. Potočnik, P. J. Baker, Y. Ohishi, M. T. McDonald, M. D. Tzirakis, A. Mclennan, G. R. Darling, M. Takata, M. J. Rosseinsky and K. Prassides, *Nature*, 2010, **466**, 221.
11 (*a*) H. Moriyama, H. Kobayashi, A. Kobayashi and T. Watanabe, *J. Am. Chem. Soc.*, 1993, **115**, 1185; (*b*) H. Kobayashi, H. Tomita, H. Moriyama, A. Kobayashi and T. Watanabe, *J. Am. Chem. Soc.*, 1994, **116**, 3153; (*c*) H. Moriyama, M. Abe, H. Motoke, T. Watanabe, S. Hayashi and H. Kobayashi, *Synth. Met.*, 1998, **94**, 167.
12 P. W. Stephens, D. Cox, J. W. Lauher, L. Mihaly, J. B. Wiley, P.-M. Allemand, A. Hirsch, K. Holczer, Q. Li, J. D. Thompson and F. Wudl, *Nature*, 1992, **355**, 331.
13 K. Kokubo, R. S. Arastoo, T. Oshima, C. C. Wang, Y. Gao, H. L. Wang, H. Geng and L. Y. Chiang, *J. Org. Chem.*, 2010, **75**, 4574.
14 C. A. Reed and R. D. Bolskar, *Chem. Rev.*, 2010, **100**, 1075.
15 Y. Marcus and G. Hefter, *Chem. Rev.*, 2006, **106**, 4585.
16 T. Oshima, T. Mikie, N. Ikuma and H. Yakuma, *Org. Biomol. Chem.*, 2010, **10**, 1730.
17 H. F. Friedman and B. Larsen, *J. Chem. Phys.*, 1979, **70**, 92.

 

JACS
JOURNAL OF THE AMERICAN CHEMICAL SOCIETY
Article
pubs.acs.org/JACS

# Kinetic Study of the Diels–Alder Reaction of $Li^+@C_{60}$ with Cyclohexadiene: Greatly Increased Reaction Rate by Encapsulated $Li^+$

Hiroshi Ueno,[†,⊥] Hiroki Kawakami,[‡] Koji Nakagawa,[†] Hiroshi Okada,[‡] Naohiko Ikuma,[†] Shinobu Aoyagi,[§] Ken Kokubo,*[,†] Yutaka Matsuo,*[,‡] and Takumi Oshima[†]

[†]Division of Applied Chemistry, Graduate School of Engineering, Osaka University, Suita, Osaka 565-0871, Japan
[‡]Department of Chemistry, School of Science, The University of Tokyo, Bunkyo-ku, Tokyo 113-0033, Japan
[§]Department of Information and Biological Sciences, Nagoya City University, Nagoya 467-8501, Japan

Supporting Information

**ABSTRACT:** We studied the kinetics of the Diels–Alder reaction of $Li^+$-encapsulated [60]fullerene with 1,3-cyclohexadiene and characterized the obtained product, [$Li^+@C_{60}(C_6H_8)$]($PF_6^-$). Compared with empty $C_{60}$, $Li^+@C_{60}$ reacted 2400-fold faster at 303 K, a rate enhancement that corresponds to lowering the activation energy by 24.2 kJ $mol^{-1}$. The enhanced Diels–Alder reaction rate was well explained by DFT calculation at the M06-2X/6-31G(d) level of theory considering the reactant complex with dispersion corrections. The calculated activation energies for empty $C_{60}$ and $Li^+@C_{60}$ (65.2 and 43.6 kJ $mol^{-1}$, respectively) agreed fairly well with the experimentally obtained values (67.4 and 44.0 kJ $mol^{-1}$, respectively). According to the calculation, the lowering of the transition state energy by $Li^+$ encapsulation was associated with stabilization of the reactant complex (by 14.1 kJ $mol^{-1}$) and the [4 + 2] product (by 5.9 kJ $mol^{-1}$) through favorable frontier molecular orbital interactions. The encapsulated $Li^+$ ion catalyzed the Diels–Alder reaction by lowering the LUMO of $Li^+@C_{60}$. This is the first detailed report on the kinetics of a Diels–Alder reaction catalyzed by an encapsulated Lewis acid catalyst rather than one coordinated to a heteroatom in the dienophile.

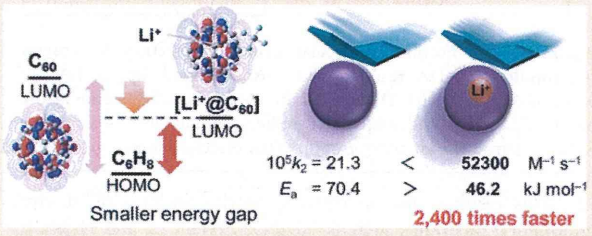


## INTRODUCTION

Since the discovery of the Diels–Alder (DA) reaction in 1928,[1] it has become the most widely studied pericyclic reaction because of its practical importance and fundamental interest in synthetic and theoretical organic chemistry.[2] According to the Woodward–Hoffmann rules, a normal-electron-demand DA reaction is a thermally allowed [4 + 2] cycloaddition that occurs through frontier molecular orbital (FMO) interactions between the HOMO of the diene and the LUMO of the dienophile. It is well-known that a smaller energy gap between the HOMO of the diene and the LUMO of dienophile often results in a higher reaction rate. A common strategy for accelerating normal-electron-demand DA reactions is to introduce an electron-donating group to the diene and/or an electron-withdrawing group to the dienophile. Another approach is Lewis acid (LA) catalysis. A heteroatom in the dienophile can serve as a coordination site for an LA, which can accelerate the DA reaction by lowering the LUMO of the dienophile (Figure 1a).[3] For example, DA reactions run in the presence of lithium ion ($Li^+$), which serves as an LA, are accelerated up to 9-fold when acrylonitrile is used as the dienophile.[4] However, metal ions cannot be used as LA catalysts in DA reactions unless the dienophile contains a heteroatom that can serve as a coordination site. In addition, steric interactions between the reactants affect the reaction rate. Yet, in previous research on the DA reaction,[3c] it has been difficult to separate the electronic and steric effects because electron-withdrawing and -donating groups inevitably have some steric effect. If electronic effects could be isolated from steric effects, this would provide useful information about the DA reaction.

The DA reaction can be used to synthesize fullerene-based n-type materials for organic photovoltaics, for example, indene-$C_{60}$ bis-adduct and methano/indene fullerenes.[5] However, the inherent equilibrium between the DA and retro-DA reactions lowers the yield and limits the scope of dienes that can be used.[6] Considering the enhancement of the DA reaction by LA activation of dienophiles, we have focused on the DA reaction of lithium-ion-encapsulated [60]fullerene $Li^+@C_{60}$.[7] Compared with empty $C_{60}$, $Li^+@C_{60}$ has a lower LUMO level[7a] but exactly the same size. When comparing the DA reactions of $C_{60}$ and $Li^+@C_{60}$, the steric effects can therefore be ignored when considering the reaction kinetics and thermodynamics, and in particular, the reaction rate can be considered in terms of only the $HOMO_{diene}$–$LUMO_{dienophile}$ gap (Figure 1b). In our previous study,[8] we used cyclopentadiene as a diene to efficiently synthesize the DA adduct of $Li^+@C_{60}$, and we observed a drastic rate enhancement due to the encapsulated

**Received:** June 13, 2014
**Published:** July 9, 2014

   dx.doi.org/10.1021/ja505952y | J. Am. Chem. Soc. 2014, 136, 11162–11167

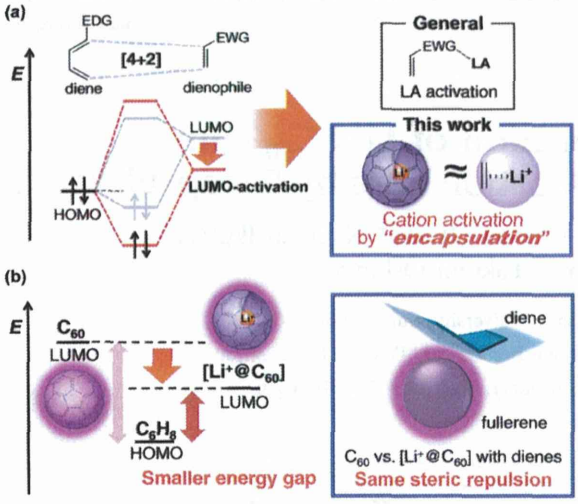


**Figure 1.** (a) Frontier molecular orbital interaction in normal-electron-demand DA reaction and DA activation by an LA and encapsulated ion. (b) Differences in electronic and steric factors between $Li^+@C_{60}$ and empty $C_{60}$ influenced the DA reaction rate. EWG, electron-withdrawing group; EDG, electron-donating group.

$Li^+$. This result stands in contrast to the findings on neutral endohedral fullerenes such as $He@C_{60}$, $H_2@C_{60}$, and $H_2@C_{70}$, which are not known to enhance reactivity of the DA reactions.[9] However, because the DA reaction of $Li^+@C_{60}$ with cyclopentadiene was extremely fast, we were unable to conduct a quantitative analysis of the kinetics.[8] This can be seen by comparing the second-order rate constants ($k_2$) for the DA reaction of empty $C_{60}$ with cyclopentadiene ($1.70 \times 10^{-1}$ $M^{-1}$ $s^{-1}$) and 1,3-cyclohexadiene ($6.71 \times 10^{-5}$ $M^{-1}$ $s^{-1}$) in toluene at 30 °C, as shown in Supporting Information Table S2.

In this study, we kinetically and computationally investigated the DA reaction of $Li^+@C_{60}$ with 1,3-cyclohexadiene ($C_6H_8$) and precisely determined the activation energy $E_a$ and other kinetic parameters. Together with the reported DA reactivity of other endohedral metallofullerenes,[10] our observed kinetics data on the DA reaction of $Li^+@C_{60}$ will provide basic knowledge that should be useful for the chemical functionalization of endohedral fullerenes and, more generally, for the understanding of DA chemistry. Our results suggest that $Li^+@C_{60}$ will be useful as a core unit of functionalized nanomaterials in organic electronics and medicinal chemistry.[11]

## RESULTS AND DISCUSSION

**Synthesis and Characterization of the DA Adduct of $Li^+@C_{60}$ and 1,3-Cyclohexadiene.** To study the kinetics of the DA reaction, we chose 1,3-cyclohexadiene ($C_6H_8$) because of its simple structure and suitable reactivity toward both $C_{60}$ and $Li^+@C_{60}$. In our experiments, the second-order rate constants for DA reactions of empty $C_{60}$ with various 1,3-dienes at 303 K were distributed over a wide range: $k_2 = 1.8 \times 10^{-5}$ to $1.7 \times 10^{-1}$ $M^{-1}$ $s^{-1}$ (Supporting Information Table S2). All reactions were carried out in the dark (Scheme 1). Reaction progress was monitored by an HPLC technique using an electrolyte-containing mobile phase,[8,11] and the monoadduct product was isolated by preparative HPLC. The product $[Li^+@C_{60}(C_6H_8)](PF_6^-)$ was very stable in solution, and no retro-DA reaction or decomposition occurred, even under heating at 383 K for 24 h. Such stability of $Li^+@C_{60}$-based DA products stands

**Scheme 1. DA Reaction of $[Li^+@C_{60}](PF_6^-)$ with 1,3-Cyclohexadiene[a]**

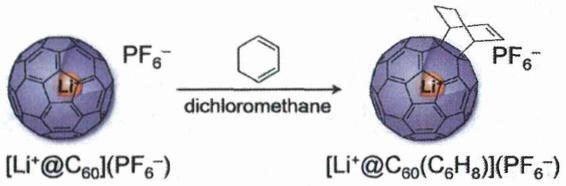


[a]10 equiv for preparation and 100 equiv for kinetic measurement.

in marked contrast to the instability of typical DA adducts of empty $C_{60}$. This comparatively high stability is ascribed to the stronger interaction between the lower lying LUMO of $Li^+@C_{60}$ and the HOMO of $C_6H_8$ (see Figure 1).[12]

The product was characterized by $^1H$, $^{13}C$, and $^7Li$ NMR, high-resolution atmospheric pressure chemical ionization time-of-flight (APCI–TOF) mass spectrometry, and single-crystal X-ray structural analysis. The $^1H$ and $^{13}C$ NMR spectra of the product (Supporting Information Figures S1 and S2) were quite similar to those of empty $C_{60}(C_6H_8)$ and showed that the product had $C_s$-symmetry with a [6,6]-addition pattern.[13] The $^7Li$ NMR spectrum (Supporting Information Figure S3) showed a single sharp signal at −13.5 ppm, indicating that the $Li^+$ was located within the highly shielded fullerene cage. This signal was shifted slightly upfield compared with that of the starting material, $[Li^+@C_{60}](PF_6^-)$,[7] because the magnetic field inside the cage is altered in the 6,6-adducts of $C_{60}$ derivatives; similar upfield shifts have been reported for $^3He$ and/or $H_2$-encapsulated 6,6-adducts of $C_{60}$ derivatives.[14] The high-resolution APCI–TOF mass spectrum showed the formation of a product at $m/z$ 807.0773, which was assigned to the molecular ion ($M^+$; calcd for $C_{66}H_8Li$, 807.0786; Supporting Information Figure S4). The UV–vis spectrum of $[Li^+@C_{60}(C_6H_8)](PF_6^-)$ was similar to that of the empty analogue (Supporting Information Figure S5).[13a] Finally, the structure was confirmed by X-ray structural analysis (Figure 2

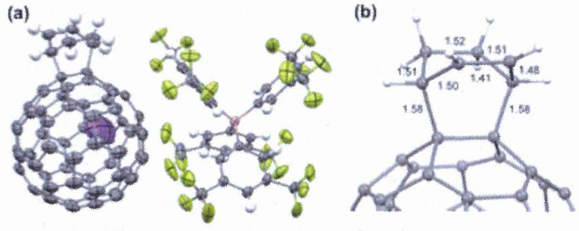


**Figure 2.** Crystal structure of $[Li^+@C_{60}(C_6H_8)]TFPB^-$: (a) $Li^+@C_{60}(C_6H_8)$ cation in the crystal; (b) $C_6H_8$ moiety on the fullerene cage (values are C–C bond lengths in angstroms).

and Supporting Information Table S1) after exchanging $PF_6^-$ with tetrakis[3,5-bis(trifluoromethyl)phenyl]borate ($TFPB^-$, $B[C_6H_3(CF_3)_2]_4^-$) by our reported procedure.[15] The crystal structure showed that the addition of $C_6H_8$ to the $C_{60}$ cage occurred at the [6,6]-bond, as has been discussed in quantum mechanical studies.[16] The encapsulated $Li^+$ was located close to a six-membered ring near one of the $C_6H_3(CF_3)_2$ groups of the TFPB counteranion.[7a]

**Kinetics of the DA Reaction of $Li^+@C_{60}$ with 1,3-Cyclohexadiene.** We studied the kinetics of the DA reaction under pseudo-first-order conditions, using a large excess of


dx.doi.org/10.1021/ja505952y | J. Am. Chem. Soc. 2014, 136, 11162–11167

$C_6H_8$ (100 equiv) at 253, 263, and 273 K for $Li^+@C_{60}$ in dichloromethane ($CH_2Cl_2$) and at 353, 363, and 373 K for empty $C_{60}$ in *o*-dichlorobenzene (*o*-DCB). Different solvents were used due to temperature limitations. We confirmed that empty $C_{60}$ exhibited no remarkable difference in kinetics between the solvents (measured at 303 K, Supporting Information Table S3). The representative HPLC profile of the DA reaction between $Li^+@C_{60}$ and $C_6H_8$ in $CH_2Cl_2$ is shown in Figure 3. The second-order rate constant $k_2$ was

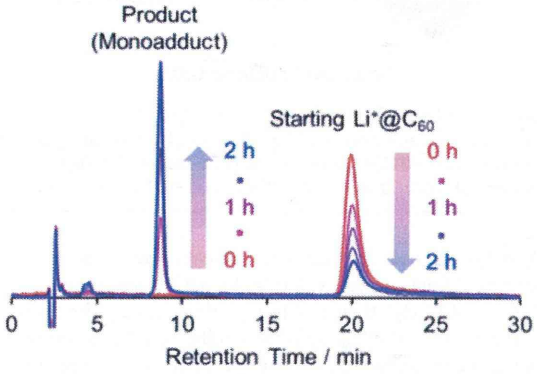


**Figure 3.** Representative HPLC profile (Buckyprep, *o*-DCB/MeCN = 9/1 with 50 mM $^n$Bu$_4$NPF$_6$, 1 mL/min) of the DA reaction of [$Li^+@C_{60}$]($PF_6^-$) with 1,3-cyclohexadiene in $CH_2Cl_2$ at 263 K in the dark.

calculated by using the measured pseudo-first-order rate constant $k'$ (Supporting Information Figure S6) from the HPLC data, according to the following equation:[17]

$$-d[Li^+@C_{60}]/dt = k'[Li^+@C_{60}] = k_2[Li^+@C_{60}][C_6H_8]$$

The $k_2$ values at various temperatures are listed in Table 1 along with the $k_2$ values estimated at 303 K by extrapolation in

**Table 1. Second-Order Rate Constants for DA Reactions of [$Li^+@C_{60}$]($PF_6^-$) and Empty $C_{60}$ with $C_6H_8$**

| [$Li^+@C_{60}$]($PF_6^-$) | | empty $C_{60}$ | |
|---|---|---|---|
| Temp./K | $10^5k_2/M^{-1}$ s$^{-1}$ | Temp./K | $10^5k_2/M^{-1}$ s$^{-1}$ |
| 253 | 1344 | 353 | 1187 |
| 263 | 3129 | 363 | 2167 |
| 273 | 6714 | 373 | 4302 |
| 303 | 52300[a] | 303 | 21.3[a] |

[a]Estimated by extrapolation in Arrhenius plot.

Arrhenius plots (Figure 4). The $k_2$ ratio ($Li^+@C_{60}$ vs $C_{60}$ at 303 K) revealed that the DA reaction of [$Li^+@C_{60}$]($PF_6^-$) was about 2400-fold faster than the reaction of empty $C_{60}$. This difference can be attributed to the encapsulated $Li^+$. Using the kinetics data, we computed the activation energy $E_a$, activation enthalpy $\Delta H^‡$, activation entropy $\Delta S^‡$, and activation Gibbs free energy $\Delta G^‡$ from Arrhenius plots ($\ln k_2$ vs $1/T$) and Eyring plots ($\ln(k_2/T)$ vs $1/T$) (see Table 2 and Figure 4) by using the following equations, respectively:[18]

$$\ln k_2 = -E_a/RT + \ln A$$

$$\ln(k_2/T) = -\Delta H^‡/RT + [\ln(k_B/h) + \Delta S^‡/R]$$

Here, $\ln A$ is a constant, $k_B$ is the Boltzmann constant, and $h$ is the Planck constant. Because the DA reaction is bimolecular,

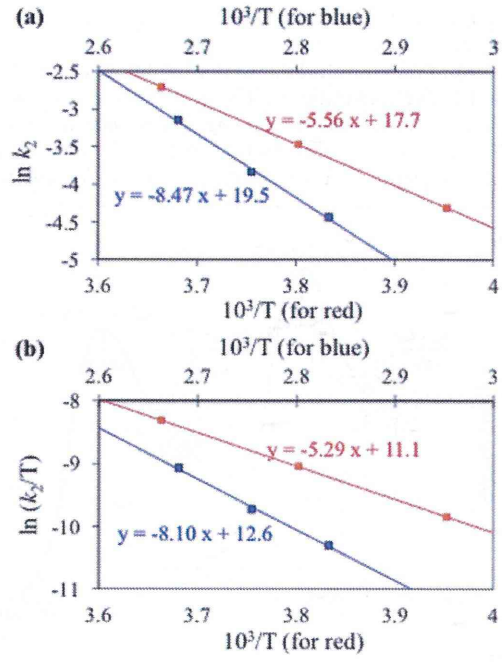


**Figure 4.** (a) Arrhenius and (b) Eyring plots in the DA reaction of [$Li^+@C_{60}$]($PF_6^-$) (red) and empty $C_{60}$ (blue) with 1,3-cyclohexadiene.

**Table 2. Activation Parameters for DA Reactions of [$Li^+@C_{60}$]($PF_6^-$) and Empty $C_{60}$ with $C_6H_8$**

| | $E_a$ kJ mol$^{-1}$ | $\Delta H^‡$ kJ mol$^{-1}$ | $\Delta S^‡$ J mol$^{-1}$ K$^{-1}$ | $\Delta G^{‡a}$ kJ mol$^{-1}$ |
|---|---|---|---|---|
| $Li^+@C_{60}$ | 46.2 | 44.0 (43.6)[b] | −381 | 144 |
| empty $C_{60}$ | 70.4 | 67.4 (65.2)[b] | −368 | 201 |

[a]The activation free energies $\Delta G^‡$ were estimated from each $\Delta H^‡$, $\Delta S^‡$, and temperature $T$ (263 K for $Li^+@C_{60}$ and 363 K for empty $C_{60}$). [b]Calculated value at M06-2X/6-31G(d) level as $E$ (thermal) at 298 K.

$\Delta S^‡$ is negative. However, there was no entropic difference between $Li^+@C_{60}$ and empty $C_{60}$. The observed $E_a$ value for the DA reaction of $Li^+@C_{60}$ with $C_6H_8$ (46.2 kJ mol$^{-1}$) was about 24 kJ mol$^{-1}$ lower than that for the reaction of empty $C_{60}$ (70.4 kJ mol$^{-1}$). This was mainly because the lower LUMO level of $Li^+@C_{60}$ strengthened the FMO interactions, which is a well-known phenomenon in LA-mediated DA reactions,[2] and we therefore attribute the observed rate enhancement to a similar effect of encapsulated $Li^+$. In general, the dominant factors in the rate constant of DA reactions are the energy difference between the HOMO of the diene and the LUMO of dienophile and the steric environment surrounding the FMOs of the diene and dienophile.[5d]

In our experiment, because $Li^+@C_{60}$ and empty $C_{60}$ have a [60]fullerene cage of nearly identical size, steric effects do not produce any difference in kinetic behavior. The present reaction is a rare example where we can discuss electronic effects alone in regard to the DA reaction rate, without considering steric effects. Furthermore, in this reaction, the encapsulated $Li^+$ is considered to be an *intramolecular catalyst*,[11a] which is also a rare example showing the effect of


dx.doi.org/10.1021/ja505952y | J. Am. Chem. Soc. 2014, 136, 11162−11167

encapsulation of an LA catalyst rather than coordination to a heteroatom.

**Computational Studies on the DA Reaction of $Li^+@C_{60}$ with 1,3-Cyclohexadiene.** The observed rate enhancement of the DA reaction was in good agreement with the results of DFT calculation at the M06-2X/6-31G(d) level including Grimme's dispersion correction[19] (Figure 5). As reported by

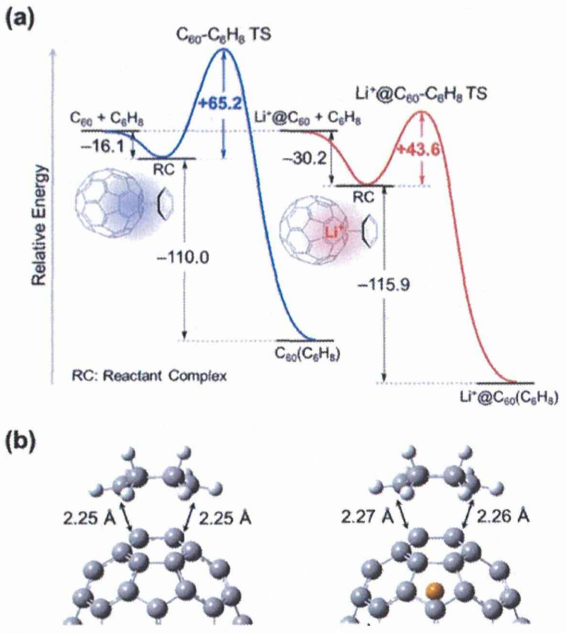


**Figure 5.** (a) Energy profiles (in kJ $mol^{-1}$) for the DA reaction of empty $C_{60}$ (blue) and $Li^+@C_{60}$ (red) with $C_6H_8$ calculated by DFT (M06-2X/6-31G(d)). (b) Transition state structures of $C_{60}$–$C_6H_8$ (left) and $Li^+@C_{60}$–$C_6H_8$ systems (right).

Osuna et al.,[16b,19] both $C_{60}$ and $Li^+@C_{60}$ form somewhat stable intermediate reactant complexes (RCs) with $C_6H_8$. Here, the calculated energy difference between the RC and transition state (TS) indicated that the activation energy for the DA reaction of $Li^+@C_{60}$ was 21.6 kJ $mol^{-1}$ lower than that of empty $C_{60}$. The calculated activation energy $E$(thermal) of 65.2 kJ $mol^{-1}$ for $C_{60}$ and 43.6 kJ $mol^{-1}$ for $Li^+@C_{60}$ agreed fairly well with the experimental values shown in Table 2: 67.4 and 44.0 kJ $mol^{-1}$, respectively. The values calculated by using the B3LYP/6-31G* level of theory without considering the RC were overestimated as 91 and 56 kJ $mol^{-1}$ (see Supporting Information Figure S7).

In addition, the calculated energy difference between the substrates and the products suggested further stabilization of $Li^+@C_{60}(C_6H_8)$, being explained by the energy gained in orbital interactions, $\Delta E$, according to Klopman–Salem equation:[12]

$$\Delta E = 2(C_aC_b\beta_{ab})^2/|e_a - e_b|$$
$$= \text{constant} \times (C_aC_b)^2/|e_a - e_b|$$

Here, $C_aC_b$ denotes the overlap of molecular orbital coefficients of interacting atomic orbitals. The term $\beta_{ab}$ is the resonance integral that converts the efficiency of overlap to units of energy. Figure 6 shows calculated LUMO energy ($e_a$) of each fullerene and the HOMO energy ($e_b$) of cyclohexadiene (M06-2X/6-31G(d)) along with schematic images of their orbitals. Because $Li^+@C_{60}$ has a lower LUMO level (closer to the HOMO of $C_6H_8$) than empty $C_{60}$, thus making the term $|e_a - e_b|$ smaller for $Li^+@C_{60}$ than for empty $C_{60}$, $\Delta E$ is increased to give a more stabilized TS and product in the case of $Li^+@C_{60}(C_6H_8)$, as shown in Figure 5 (115.9 kJ $mol^{-1}$ from the RC and 146.1 kJ $mol^{-1}$ from the starting material). In the case of empty $C_{60}$, these values are somewhat smaller: 110.0 and 126.1 kJ $mol^{-1}$, respectively. The reason for the formation of the more stable RC from $Li^+@C_{60}$ than from $C_{60}$ is also attributable to the same FMO interactions.

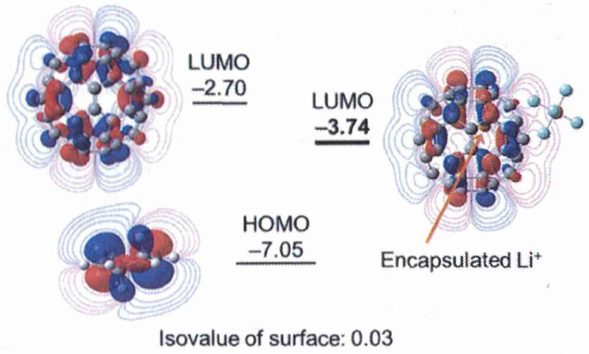


**Figure 6.** Calculated LUMOs of $Li^+@C_{60}$ (with $PF_6^-$ counteranion) and empty $C_{60}$, and calculated HOMO of $C_6H_8$ with energies (eV) at the M06-2X/6-31G(d) level. Contour lines in the figure indicate isovalues of 0.001, 0.002, 0.004, 0.008, and 0.02 from the outer side.

As shown in Figure 6, the slightly delocalized LUMO of $Li^+@C_{60}$, and thus its increased LUMO coefficient $C$, could be another factor in increasing $\Delta E$. The slightly increased partial charges in the RC and TS ($\delta-$ at the electron-accepting fullerenyl carbon and $\delta+$ at the electron-donating $C_6H_8$ carbon) could be stabilized by the inner $Li^+$ of $Li^+@C_{60}$. This may be the reason that $C_6H_8$ approaches $Li^+@C_{60}$ from the $Li^+$ side in the TS (Figure 5). These electronic effects can be quantitatively discussed when steric effect can be completely ignored. In the present comparison of DA kinetics, our system is clearly the ideal case where only electronic effects need to be considered and steric effects can be ignored.

## ■ CONCLUSION

In summary, we have synthesized and characterized a new $Li^+$-encapsulated fullerene derivative $[Li^+@C_{60}(C_6H_8)](PF_6^-)$ obtained by the DA reaction of $[Li^+@C_{60}](PF_6^-)$ with 1,3-cyclohexadiene. Our study of the DA reaction kinetics revealed that $Li^+@C_{60}$ reacted about 2400 times faster than empty $C_{60}$, because of the stronger interaction between the lower-lying LUMO of $Li^+@C_{60}$ with the HOMO of cyclohexadiene. This remarkable rate enhancement was explained by encapsulated $Li^+$ lowering the activation energy by 24 kJ $mol^{-1}$, as estimated from Arrhenius plots. Values of other kinetic parameters, namely, activation enthalpy $\Delta H^{\ddagger}$, activation entropy $\Delta S^{\ddagger}$, and activation Gibbs free energy $\Delta G^{\ddagger}$, were obtained from Eyring plots. The observed rate enhancement caused by encapsulated $Li^+$ was supported by DFT calculation at the M06-2X/6-31G(d) level of theory considering RCs with dispersion corrections. The calculation results suggest that encapsulation of $Li^+$ lowered the activation energy by 21.6 kJ $mol^{-1}$, which was consistent with the experimental value. The activation energy was lowered through stabilization of the RC and the [4


dx.doi.org/10.1021/ja505952y | J. Am. Chem. Soc. 2014, 136, 11162–11167

+ 2] product by 14.1 and 5.9 kJ $mol^{-1}$, respectively. We conclude that encapsulated $Li^+$ clearly caused the drastic rate enhancement. In this study, we have successfully examined the relation between the $HOMO_{diene}$–$LUMO_{dienophile}$ energy gap and DA reaction rate, while isolating the electronic effects and excluding the steric effects.

## EXPERIMENTAL SECTION

**General Procedure.** $[Li^+@C_{60}](PF_6^-)$ was obtained from Idea International Corporation. All other reagents were commercially available and used without further purification. High resolution mass spectra were obtained by APCI using a TOF mass analyzer on a JEOL JMS-T100LC (AccuTOF) spectrometer with a calibration standard of polyethylene glycol (MW 1000). The $^7Li$, $^1H$, and $^{13}C$ NMR spectra were recorded at 233.12, 599.85, and 150.84 MHz on a Varian Unity Inova 600. UV–vis spectra were recorded on a Shimadzu UV-1800 spectrometer.

**Synthesis of $[Li^+@C_{60}(C_6H_8)](PF_6^-)$.** 1,3-Cyclohexadiene (dichloromethane solution, 53.7 mM, 2 mL, 107 μmol) was slowly added to a dichloromethane solution (47 mL) of $[Li^+@C_{60}]PF_6^-$ (9.37 mg, 10.7 μmol) and reacted at 0 °C for 150 min. Then unreacted 1,3-cyclohexadiene was removed in vacuo after dilution of the crude solution by adding chlorobenzene (30 mL) to avoid further progress of the reaction in this process. The product was purified by HPLC at 30 °C using a πNAP (Nacalai Tesque COSMOSIL 4.6 × 250 nm); the mobile phase was chlorobenzene/1,2-dichloroethane/acetonitrile = 2/1.5/6.5 (v/v/v) saturated with $Me_4NPF_6$. After evaporating the solvent in vacuo, dichloromethane was added to the red–brown residue containing white solids of $Me_4NPF_6$. After removing the solids by filtration, recrystallization from the solution by vapor-diffusion with diethyl ether at 0 °C gave brown crystals of $[Li^+@C_{60}(C_6H_8)]PF_6^-$ (1.8 mg, 18%, 1.9 μmol, red–brown solid). $^1H$ NMR (600 MHz, dichloromethane-$d_2$): δ 7.34 (dd, $J$ = 4.6, 3.2 Hz, 2H, vinyl), 4.26 (m, 2H, bridgehead), 3.10 (m, 2H), 2.31 (m, 2H). $^{13}C$ NMR (151 MHz, dichloromethane-$d_2$): δ 156.88 (s), 156.24 (s), 146.46 (s), 145.54 (s), 145.46 (s), 145.31 (s), 145.28 (s), 145.16 (s), 144.81 (s), 144.49 (s), 144.47 (s), 144.35 (s), 144.07 (s), 143.54 (s), 143.29 (s), 142.43 (s), 142.07 (s), 141.92 (s), 141.07 (s), 140.78 (s), 140.77 (s), 140.68 (s), 140.63 (s), 140.57 (s), 139.00 (s), 138.94 (s), 136.38 (s), 135.40 (s), 135.14 (s), 70.48 (s), 42.87 (s), 24.59 (s). $^7Li$ NMR (233 MHz, dichloromethane-$d_2$): δ −13.5 (s). High-resolution APCI-TOF MS (+): $m/z$ calcd for $C_{66}H_8Li$, 807.0786; found, 807.0773.

**X-ray Structural Analysis of $[Li^+@C_{60}(C_6H_8)]TFPB^-$.** Structural characterization of $Li^+@C_{60}(C_6H_8)$ was performed by means of single crystal X-ray diffraction of $[Li^+@C_{60}(C_6H_8)]TFPB^-$. $[Li^+@C_{60}(C_6H_8)]PF_6^-$ (0.2 mg) and NaTFPB (1.1 mg, excess) were dissolved in 4 mL of dichloromethane with ultrasonic agitation (1 min). Then, the solution was filtered and concentrated in vacuo to ~60 μL. Recrystallization from the solution by vapor-diffusion with diethyl ether at 0 °C gave brown crystals of $[Li^+@C_{60}(C_6H_8)]TFPB^-$. The synchrotron-radiation X-ray diffraction measurement was performed by using the large cylindrical image-plate camera at SPring-8 BL02B1 (Hyogo, Japan) at 150 K. The crystal structure analysis was performed by using *SHELX*. The results are summarized in Supporting Information Table S1 and the CIF file (CCDC 985137). The $Li^+@C_{60}(C_6H_8)$ crystal showed a disordered structure with two molecular orientations evenly coexisted in the crystal. The encapsulated $Li^+$ cation is localized under a six-membered ring so that the $C_s$ symmetry of the molecule is broken in the crystal.

**Kinetic Evaluation in the DA Reactions of $[Li^+@C_{60}](PF_6^-)$ and Empty $C_{60}$ with 1,3-Cyclohexadiene (and Other 1,3-Dienes).** The kinetic measurements for the DA reactions of $[Li^+@C_{60}](PF_6^-)$ and empty $C_{60}$ with 1,3-cyclohexadiene were performed under pseudo-first-order conditions by using a large excess of diene (ca. 100 equiv, 6 mM) relative to fullerenes (ca. 60 μM) in the dark. The progress of the reaction was followed by monitoring the consumption of $C_{60}$ by HPLC. For $[Li^+@C_{60}](PF_6^-)$: column, Buckyprep (Nacalai Tesque COSMOSIL 4.6 × 250 nm); eluent, *o*-dichlorobenzene/acetonitrile = 9/1 (v/v) with saturated $^nBu_4NPF_6$; temperature, RT. For empty $C_{60}$; column: Buckyprep (Nacalai Tesque COSMOSIL 4.6 × 250 nm), eluent: toluene, temperature: RT. Monitoring the reaction by HPLC showed a gradual increase of monoadduct ($[Li^+@C_{60}(C_6H_8)](PF_6^-)$ or empty $C_{60}(C_6H_8)$) accompanied by consumption of the starting material. The natural logarithmic plot of the normalized signal intensity of each remaining fullerene starting material (relative to the signal intensity of the first aliquot at $t$ = 0) was linear with respect to time. The obtained slope, that is, the pseudo-first-order rate constant $k'$, was divided by the concentration of 1,3-cyclohexadiene to obtain the second-order rate constants $k_2$.

**Theoretical Calculation.** Full geometry optimizations have been carried out by using the restricted M06-2X functional with the 6-31G(d) basis set in *Gaussian 09* (rev. C.01) software.[20] Frequency calculations showed only one imaginary frequency for the transition states (351*i* for $Li@C_{60}^+$ and 404*i* for $C_{60}$) or no imaginary frequency for the other states. All energies include zero-point energies (ZPEs) and thermal corrections by the frequency calculations.

## ASSOCIATED CONTENT

### Supporting Information

Crystallographic data (including CIF), kinetic data with various 1,3-dienes and in various solvents, spectroscopic data (NMR, MS, and UV–vis) of the new compound, kinetic plots of the DA reactions, the calculated energy profiles at B3LYP/6-31G* level, the calculated energies, and the coordinates of the atoms in all the molecules optimized. This material is available free of charge via the Internet at http://pubs.acs.org.

## AUTHOR INFORMATION


### Corresponding Authors

*E-mail: kokubo@chem.eng.osaka-u.ac.jp.

*E-mail: matsuo@chem.s.u-tokyo.ac.jp.

### Present Address

⊥H. Ueno: JST ERATO Itami Molecular Nanocarbon Project, Graduate School of Science, Nagoya University, Japan.


### Notes

The authors declare no competing financial interest.

## ACKNOWLEDGMENTS

This work was partly supported by Adaptable and Seamless Technology Transfer Program through target-driven R&D, JST, Health Labor Sciences Research Grants from the MHLW of Japan (to K.K.), and the Funding Program for Next-Generation World-Leading Researchers (to Y.M.). The X-ray diffraction measurement was performed at SPring-8 with the approval of the Japan Synchrotron Radiation Research Institute (JASRI) (Proposal No. 2013B0100).

## REFERENCES

(1) Diels, O.; Alder, K. *Liebigs Ann. Chem.* **1928**, *460*, 98–122.

(2) Jiang, X.; Wang, R. *Chem. Rev.* **2013**, *113*, 5515–5546.

(3) (a) Pham, H. V.; Paton, R. S.; Ross, A. G.; Danishefsky, S. J.; Houk, K. N. *J. Am. Chem. Soc.* **2014**, *136*, 2397–2403. (b) Konovalov, A. I.; Kiselev, V. D. *Russ. Chem. Bull., Int. Ed.* **2003**, *52*, 293–311. (c) Sustmann, R.; Schubert, R. *Angew. Chem., Int. Ed.* **1972**, *11*, 840–840.

(4) (a) Forman, M. A.; Dailey, W. P. *J. Am. Chem. Soc.* **1991**, *113*, 2761–2762. (b) Tsuda, A.; Oshima, T. *New J. Chem.* **1998**, 1027–1029.

(5) (a) Hudhomme, P. *C. R. Chimie* **2006**, *9*, 881–891. (b) Matsuo, Y.; Kawai, J.; Inada, H.; Nakagawa, T.; Ota, H.; Otsubo, S.; Nakamura, E. *Adv. Mater.* **2013**, *25*, 6266–6269. (c) He, Y.; Chen, H.-Y.; Hou, J.; Li, Y. *J. Am. Chem. Soc.* **2010**, *132*, 1377–1382. (d) Ikuma, N.; Susami, Y.; Oshima, T. *Eur. J. Org. Chem.* **2011**, 6452–6458.

(6) (a) Schlueter, J. A.; Seaman, J. M.; Taha, S.; Cohen, H.; Lykke, K. R.; Wang, H. H.; Williams, J. M. *J. Chem. Soc., Chem. Commun.* **1993**, 972–974. (b) Komatsu, K.; Murata, Y.; Sugita, N.; Takeuchi, K.; Wan, T. S. M. *Tetrahedron Lett.* **1993**, *34*, 8473–8476. (c) Giovane, L. M.; Barco, J. W.; Yadav, T.; Lafleur, A. L.; Marr, J. A.; Howard, J. B.; Rotello, V. M. *J. Phys. Chem.* **1993**, *97*, 8560–8561.

(7) (a) Aoyagi, S.; Nishibori, E.; Sawa, H.; Sugimoto, K.; Takata, M.; Miyata, Y.; Kitaura, R.; Shinohara, H.; Okada, H.; Sakai, T.; Ono, Y.; Kawachi, K.; Yokoo, K.; Ono, S.; Omote, K.; Kasama, Y.; Ishikawa, S.; Komuro, T.; Tobita, H. *Nat. Chem.* **2010**, *2*, 678–683. (b) Okada, H.; Komuro, T.; Sakai, T.; Matsuo, Y.; Ono, Y.; Omote, K.; Yokoo, K.; Kawachi, K.; Kasama, Y.; Ono, S.; Hatakeyama, R.; Kaneko, T.; Tobita, H. *RSC Adv.* **2012**, *2*, 10624–10631. (c) Fukuzumi, S.; Ohkubo, K.; Kawashima, Y.; Kim, D. S.; Park, J. S.; Jana, A.; Lynch, V. M.; Kim, D.; Sessler, J. L. *J. Am. Chem. Soc.* **2011**, *133*, 15938–15941. (d) Aoyagi, S.; Sado, Y.; Nishibori, E.; Sawa, H.; Okada, H.; Tobita, H.; Kasama, Y.; Kitaura, R.; Shinohara, H. *Angew. Chem., Int. Ed.* **2012**, *51*, 3377–3381. (e) Ueno, H.; Kokubo, K.; Nakamura, Y.; Ohkubo, K.; Ikuma, N.; Moriyama, H.; Fukuzumi, S.; Oshima, T. *Chem. Commun.* **2013**, *49*, 7376–7378.

(8) Kawakami, H.; Okada, H.; Matsuo, Y. *Org. Lett.* **2013**, *15*, 4466–4469.

(9) (a) Murata, M.; Maeda, S.; Morinaka, Y.; Murata, Y.; Komatsu, K. *J. Am. Chem. Soc.* **2008**, *130*, 15800–15801. (b) Frunzi, M.; Xu, H.; Cross, R. J.; Saunders, M. *J. Phys. Chem. A* **2009**, *113*, 4996–4999. (c) Osuna, S.; Swart, M.; Solà, M. *Chem.—Eur. J.* **2009**, *15*, 13111–13123;Osuna, S.; Swart, M.; Solà, M. *Chem.—Eur. J.* **2010**, *16*, 3878–3878. (d) Osuna, S.; Swart, M.; Solà, M. *Phys. Chem. Chem. Phys.* **2011**, *13*, 3585–3603.

(10) (a) Maeda, Y.; Miyashita, J.; Hasegawa, T.; Wakahara, T.; Tsuchiya, T.; Nakahodo, T.; Akasaka, T.; Mizorogi, N.; Kobayashi, K.; Nagase, S.; Kato, T.; Ban, N.; Nakajima, H.; Watanabe, Y. *J. Am. Chem. Soc.* **2005**, *127*, 12190–12191. (b) Garcia-Borràs, M.; Luis, J. M.; Swart, M.; Solà, M. *Chem.—Eur. J.* **2013**, *19*, 4468–4479. (c) Sato, S.; Maeda, Y.; Guo, J.-D.; Yamada, M.; Mizorogi, N.; Nagase, S.; Akasaka, T. *J. Am. Chem. Soc.* **2013**, *135*, 5582–5587.

(11) (a) Matsuo, Y.; Okada, H.; Maruyama, M.; Sato, H.; Tobita, H.; Ono, Y.; Omote, K.; Kawachi, K.; Kasama, Y. *Org. Lett.* **2012**, *14*, 3784–3787. (b) Ueno, H.; Nakamura, Y.; Ikuma, N.; Kokubo, K.; Oshima, T. *Nano Res.* **2012**, *5*, 558–564. (c) Ueno, H.; Kokubo, K.; Kwon, E.; Nakamura, Y.; Ikuma, N.; Oshima, T. *Nanoscale* **2013**, *5*, 2317–2321.

(12) (a) Klopman, G. *J. Am. Chem. Soc.* **1968**, *90*, 223–234. (b) Salem, L. *J. Am. Chem. Soc.* **1968**, *90*, 543–552.

(13) (a) Kräutler, B.; Maynollo, J. *Tetrahedron* **1996**, *52*, 5033–5042. (b) Kräutler, B.; Miiller, T.; Maynollo, J.; Gruber, K.; Kratky, C.; Ochsenbein, C.; Schwarzenbach, D.; Bürgi, H.-B. *Angew. Chem., Int. Ed. Engl.* **1996**, *35*, 1204–1206.

(14) (a) Saunders, M.; Cross, R. J.; Jiménez-Vázquez, H. A.; Shimshi, R.; Khong, A. *Science* **1996**, *271*, 1693–1697. (b) Murata, M.; Murata, Y.; Komatsu, K. *J. Am. Chem. Soc.* **2006**, *128*, 8024–8033.

(15) Okada, H.; Matsuo, Y. *Fullerenes, Nanotubes, Carbon Nanostruct.* **2014**, *22*, 262–268.

(16) (a) Osuna, S.; Morera, J.; Cases, M.; Morokuma, K.; Solà, M. *J. Phys. Chem. A* **2009**, *113*, 9721–9726. (b) Fernandez, I.; Solà, M.; Bickelhaupt, F. M. *Chem.—Eur. J.* **2013**, *19*, 7416–7422.

(17) Oshima, T.; Kitamura, H.; Higashi, T.; Kokubo, K.; Seike, N. *J. Org. Chem.* **2006**, *71*, 2995–3000.

(18) (a) Eyring, H. *J. Chem. Phys.* **1935**, *3*, 107–115. (b) Pross, A. In *Theoretical and Physical Principles of Organic Reactivity*; John Wiley & Sons, Inc.: New York, 1995; pp 130–133.

(19) Osuna, S.; Marcel, S.; Solà, M. *J. Phys. Chem. A* **2011**, *115*, 3491–3496.

(20) Frisch, M. J.; Trucks, G. W.; Schlegel, H. B.; Scuseria, G. E.; Robb, M. A.; Cheeseman, J. R.; Scalmani, G.; Barone, V.; Mennucci, B.; Petersson, G. A.; Nakatsuji, H.; Caricato, M.; Li, X.; Hratchian, H. P.; Izmaylov, A. F.; Bloino, J.; Zheng, G.; Sonnenberg, J. L.; Hada, M.; Ehara, M.; Toyota, K.; Fukuda, R.; Hasegawa, J.; Ishida, M.; Nakajima, T.; Honda, Y.; Kitao, O.; Nakai, H.; Vreven, T.; Montgomery, Jr., J. A.; Peralta, J. E.; Ogliaro, F.; Bearpark, M.; Heyd, J. J.; Brothers, E.; Kudin, K. N.; Staroverov, V. N.; Kobayashi, R.; Normand, J.; Raghavachari, K.; Rendell, A.; Burant, J. C.; Iyengar, S. S.; Tomasi, J.; Cossi, M.; Rega, N.; Millam, N. J.; Klene, M.; Knox, J. E.; Cross, J. B.; Bakken, V.; Adamo, C.; Jaramillo, J.; Gomperts, R.; Stratmann, R. E.; Yazyev, O.; Austin, A. J.; Cammi, R.; Pomelli, C.; Ochterski, J. W.; Martin, R. L.; Morokuma, K.; Zakrzewski, V. G.; Voth, G. A.; Salvador, P.; Dannenberg, J. J.; Dapprich, S.; Daniels, A. D.; Farkas, Ö.; Foresman, J. B.; Ortiz, J. V.; Cioslowski, J.; Fox, D. J. *Gaussian 09*, revision C.01; Gaussian, Inc., Wallingford, CT, 2010.